Self-imaging effect in photonic crystal multimode waveguides exhibiting no band gaps

Tianbao Yu (于天宝)[1,2], Xiaoqing Jiang (江晓清)[1], Qinghua Liao (廖清华)[2], Wei Qi (戚 伟)[1], Jianyi Yang (杨建义)[1], and Minghua Wang (王明华)[1]

[1]*Department of Information Science and Electronic Engineering, Zhejiang University, Hangzhou 310027*

[2]*Department of Physics, Nanchang University, Nanchang 330047*

Received July 12, 2007

The properties of the propagating field in multimode photonic crystal waveguides (PCWs) exhibiting no photonic band gaps (PBGs) are investigated. The transmission spectrum shows that the input field can be guided with high efficiency, and resemble index-guided modes owing to the combination of total internal reflection (TIR) and distributed Bragg reflection (DBR). Self-imaging effect happens and the filling fraction determines the beating lengths. The rows of air holes decide DBR coming from the mirrors on both sides of the guiding region, which governs the transmission spectrum. It provides a new way to realize the components for both polarizations by combining PBG and TIR effects in PCWs.

OCIS codes: 130.0130, 130.2790.

Photonic crystals (PCs)[1], consisting of periodic dielectric materials, have attracted much interest in the past twenty years due to their capability to control the electromagnetic (EM) waves. Photonic crystal waveguide (PCW) is one of the most promising components of PCs in photonic integrated circuits (PICs), and the guided waves are mainly guided by photonic band gaps (PBGs) due to the existence of defect modes inside the PBGs[2]. However, the propagating field can be guided by not only the PBG effect but also total internal reflection (TIR) effect[3−6]. Multimode interference (MMI) devices are important components in PICs owing to their simple structure, low loss, and large optical bandwidth[7]. Recently, MMI effect on the basis of PBGs has been presented in the multimode PCWs[8−10]. We also discussed the MMI effect of a kind of multimode PCW, whereas the propagating modes resemble index-like modes[6].

In this letter, we present that the input field can be guided with high efficiency owing to the combination of TIR and distributed Bragg reflection (DBR), and study the effect of structure parameters on the propagating field in multimode PCWs having no PBGs. Self-imaging effect happens and the filling fraction determines the lengths of the N-fold images. The rows of air holes determine DBR and transmission spectrum.

The proposed structures are in the form of air hole arrays with a square lattice in a dielectric slab such as Si or GaAs, whose refractive index is 3.4, as shown in Fig. 1(a). The filling fraction of holes is $\mathrm{FR} = \pi(r/a)^2$, where r is the radius of the air hole and a is the lattice constant. The vertical confinement of light is characterized by use of effective index in place of the refractive index n_{eff} of the background dielectric slab in calculation[11]. An air bridge structure and a slab thickness of 250 nm are considered. The effective index of $n_{\mathrm{eff}} = 2.95$ is obtained by a beam propagation simulation[12]. Figure 1(b) shows the band diagram of transverse-magnetic (TM) modes as the filling fraction is 0.5 in perfect PCs obtained by using the plane wave expansion method[13]. It is found that there is no PBG in the dispersive curves. The modes are the extended modes, which cannot be guided along PCWs using PBGs effect. However, the EM waves can also be propagated through the index contrast[3−6].

A kind of multimode PCW is formed by removing multiple rows of air holes in the perfect PCs, as shown in Fig. 1(c). The waveguide consists of three parts: dielectric-core region (multimode region), two PCs mirrors on both sides of the core. The system is equivalent to a conventional three-layer dielectric waveguide composed of the core, the cladding, and the substrate[6]. The equivalent structure is symmetry, i.e., the refractive indices of the cladding and the substrate are uniform, due to the fact that the PC mirrors are identical. The dielectric constant of the core is the same as that of the slab. The width W_{M} of the multimode region can be considered as the multiplier of the number of rows of the removed holes and lattice constant a, and here we set W_{M} to be $5a$.

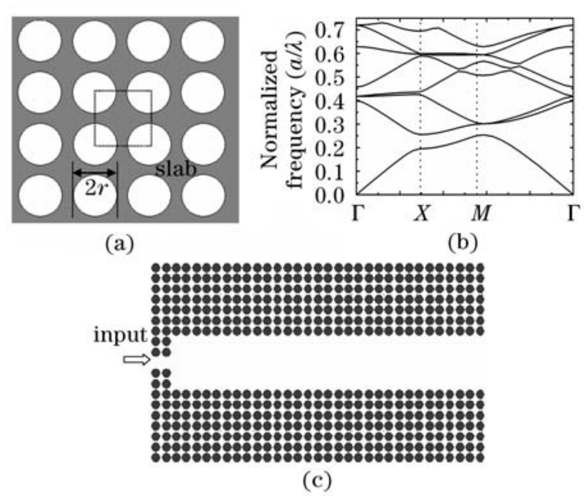

Fig. 1. (a) Air hole arrays with a square lattice in dielectric slab; (b) band diagram for TM modes; (c) schematic diagram of multimode PCWs formed by removing five rows of air holes.

The effective indices of the substrate and cladding are equal approximately to average permittivity:

$$\varepsilon_{\mathrm{ave}} = \varepsilon_{\mathrm{eff}} - \mathrm{FR}(\varepsilon_{\mathrm{eff}} - 1). \quad (1)$$

The distribution of refractive index is satisfied with TIR, and MMI effect behaves like a conventional dielectric multimode waveguide[6]. We consider the case of symmetric interference, and the positions of the first N-fold images, which is defined as the distance between the start of the multimode region and the location where the replica images are reproduced, are at $L_N = 3\pi(\beta_0 - \beta_1)/(4N)$.

Figure 2 shows the equivalent positions L_1 of the first 1-fold images of the input field as a function of the normalized frequency with different filling fractions in the three-layer multimode waveguides. The beating lengths increase linearly with the increase of operational frequencies. As the filling fraction increases, the average permittivity of the PC mirrors decreases. Accordingly the refractive index difference between the cladding and guiding regions increases, the beating length decreases, and the confinement of the light becomes stronger. Thus, it is concluded that the filling fraction of holes determines the positions of the N-fold images by controlling the index contrast between the core, the cladding, and the substrate.

The finite-difference time-domain (FDTD) method[14] with perfectly matched layers absorbing the outgoing waves is used to evaluate the efficiency of the multimode PCWs. The filling fraction is chosen to be 0.5. The position of the 1-fold image of the working point $a/\lambda = 0.44$ is $37a$ from Fig. 2. Then we construct a multimode PCW with a length of $37a$. A pulse source is launched into the model. Figure 3 shows the transmission spectrum. It is found that high transmissivity can be obtained within some wide frequency regions. Actually, there is no PBG within those frequency regions from Fig. 1(b). It implies that the propagating field can be confined tightly in the multimode PCWs by TIR effect. There are some ripples in the response spectrum in Fig. 3. This is because that there are periodic PC structures on both sides of the guiding region, which lead to DBR. Thus the combination of TIR and DBR effect determines the propagation of the guided modes. There exist some drops within the response spectrum. This means that the light with those frequencies propagates along the multimode PCWs with large loss. It can be explained by the reason as follows. The input fields may excite some modes in PCs, however, all the modes in the PC mirrors are the extended modes which are lossy and attenuate while they propagate along the multimode PCWs. Hence, the input EM waves with those frequencies are attenuated.

The rows R_{D} of the air holes located in both sides of the multimode region may cause different DBRs. We assume that the lattice constant is 0.682 μm. A pulse source for TM wave centered around 1.55 μm is also launched into the multimode PCWs with different R_{D} values. As normalized to the input powers at the entrance of the multimode PCWs, the output powers at the positions $L_1 = 37a$ of the first 1-fold image at 1.55 μm with different R_{D} values are shown in Fig. 4. When there are only three rows of air holes in mirrors, the response region with high transmittance lies within the shorter wavelength region. The transmission coefficient increases within the longer wavelength region as the rows of air holes increase. Then the spectrum becomes flatter and wider. A wide and flat response spectrum with high transmissivity (near 0.16 dB) is obtained as the rows of air holes increase to seven. It implies that the DBR plays an important role in the efficiency of the multimode PCWs dependent on TIR effect. Furthermore, more rows of holes are necessary to obtain enough DBR in the practical devices.

In conclusion, the properties of propagating field in multimode PCWs exhibiting no PBGs are investigated.

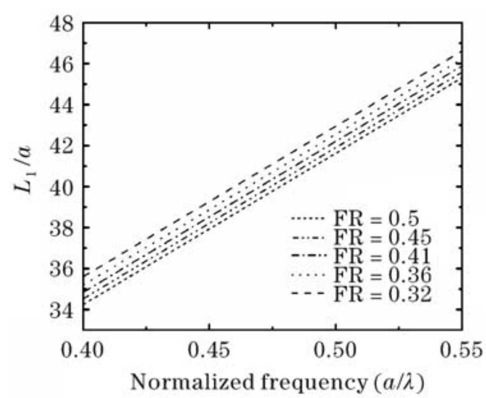

Fig. 2. Equivalent positions L_1 of the first 1-fold images of the input field as a function of the normalized frequency with different filling fractions in the three-layer multimode waveguides.

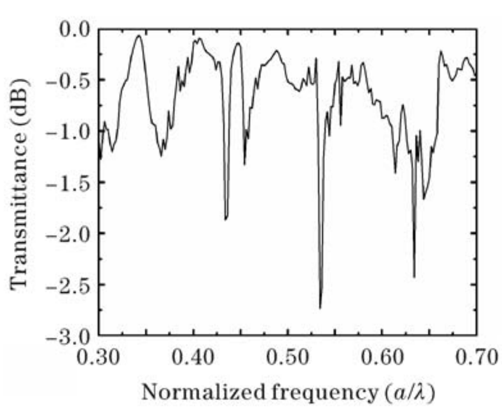

Fig. 3. Transmission spectrum of multimode PCWs with a length of $37a$.

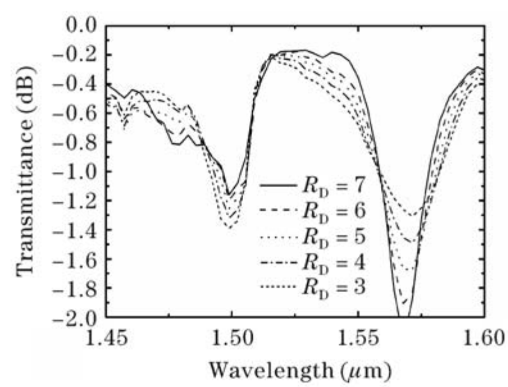

Fig. 4. Transmission efficiency of the multimode PCWs with different rows of air holes.

The equivalent conventional multimode waveguides are used to analyze the proposed structures. The combination of TIR and DBR determines the propagation of the guided modes. The filling fraction determines the beating lengths and the rows of air holes decide DBR which governs the transmission spectrum. This letter provides a novel way to design the components for all the polarizations using MMI effect in PCWs by combining TIR and PBG effects, because we may guide one kind of polarization light using TIR effect, guide another kind of polarization light using PBG effect within the interesting frequency range. The properties of MMI PCWs here may have practical applications in the integrated optics field.

This work was supported by the National Natural Science Foundation of China (No. 60477018, 10664002, and 10547119) and the Key Program of National Natural Science Foundation (No. 60436020). T. Yu's e-mail address is tbyu@zju.edu.cn.

References

1. C. M. Soukoulis, *Photonic Band Gaps and Localization* (Plenum, New York, 1993).
2. S. G. Johnson, P. R. Villeneuve, S. Fan, and J. D. Joannopoulos, Phys. Rev. B **62,** 8212 (2000).
3. A. Adibi, Y. Xu, R. K. Lee, A. Yariv, and A. Scherer, Phys. Rev. B **64,** 033308 (2001).
4. P. I. Borel, L. H. Frandsen, M. Thorhauge, A. Harpøth, Y. X. Zhuang, M. Kristensen, and H. M. H. Chong, Opt. Express **11,** 1757 (2003).
5. T. Liu, A. R. Zakharian, M. Fallahi, J. V. Moloney, and M. Mansuripur, IEEE Photon. Technol. Lett. **17,** 1435 (2005).
6. T.-B. Yu, X.-Q. Jiang, J.-Y. Yang, H.-F. Zhou, Q.-H. Liao, and M.-H. Wang, Phys. Lett. A **369,** 167 (2007).
7. L. B. Soldano and E. C. M. Pennings, J. Lightwave Technol. **13,** 615 (1995).
8. H.-J. Kim, I. Park, B.-H. O, S.-G. Park, E.-H. Lee, S.-G. Lee, Opt. Express **12,** 5625 (2004).
9. D. Modotto, M. Conforti, A. Locatelli, and C. D. Angelis, J. Lightwave Technol. **25,** 402 (2007).
10. T.-B. Yu, M.-H. Wang, X.-Q. Jiang, Q.-H. Liao, and J.-Y. Yang, J. Opt. A **9,** 37 (2007).
11. M. Qiu, Appl. Phys. Lett. **81,** 1163 (2002).
12. Y. Tanaka, H. Nakamura, Y. Sugimoto, N. Ikeda, K. Asakawa, and K. Inoue, IEEE J. Quantum Electron. **41,** 76 (2005).
13. M. Plihal and A. A. Maradudin, Phys. Rev. B **44,** 8565 (1991).
14. A. Taflove and S. C. Hagness, *Computational Electrodynamics: The Finite-Difference Time-Domain Method* (2nd end.) (Artech House, Boston, 2000).